Bayesian optimization of radical polymerization reactions in a flow synthesis system

Shogo Takasuka,*[a] Sho Ito,[a] Shunto Oikawa,[a] Yosuke Harashima,[a,b] Tomoaki Takayama,[a,b] Aniruddha Nag,[a] Araki Wakiuchi,[a,c] Tsuyoshi Ando,[a] Tetsunori Sugawara,[d] Miho Hatanaka,[e] Tomoyuki Miyao,[a,b,f] Takamitsu Matsubara,[a] Yu-ya Ohnishi,[c] Hiroharu Ajiro [a,b,f] and Mikiya Fujii *[a,b,f]

a. Graduate School of Science and Technology, Nara Institute of Science and Technology, 8916-5 Takayama-cho, Ikoma, Nara 630-0192, Japan.

b. Data Science Center, Nara Institute of Science and Technology, 8916-5 Takayama-cho, Ikoma, Nara 630-0192, Japan.

c. Materials Informatics Initiative, RD technology and digital transformation center, JSR Corporation, 3-103-9 Tonomachi, Kawasaki-ku, Kawasaki, Kanagawa 210-0821, Japan.

d. Fine Chemical Process Dept., JSR Corporation, 100 Kawajiri-cho, Yokkaichi, Mie 510-8552, Japan.

e. Department of Chemistry, Faculty of Science and Technology, Keio University, 3-14-1 Hiyoshi, Kohoku-ku, Yokohama, Kanagawa 223-8522, Japan.

f. Center for Material Research Platform, Nara Institute of Science and Technology, 8916-5 Takayama-cho, Ikoma, Nara 630-0192, Japan.

Abstract

The proportional amounts of monomers within a copolymer will greatly affect the properties of the material. However, as known as composition drift, the monomer ratio in a copolymer can deviate from the value expected from the raw material ratio due to differences in monomer reactivity. Hence, it is therefore necessary to optimize the polymerization process on the basis that this inevitable composition drift will take place. In the present study, styrene-methyl methacrylate copolymers were generated using a flow synthesis system and the processing variables were tuned employing Bayesian optimization (BO) to obtain a target composition. Initial trials employed BO to produce four candidate points per cycle, completing the optimization within five cycles, and the solvent-to-monomer ratio was identified as the most important variable. Subsequent BO tests employed 40 points per cycle and established that multiple sets of processing conditions could provide the desired composition, but with variations in the physical properties of the copolymers. The role of each variable in the radical polymerization reaction was elucidated by assessing the extensive array of processing conditions while evaluating several broad trends. The proposed model confirms that specific monomer proportions can be produced in a copolymer using machine learning while investigating the reaction mechanism. In the future, the use of multi-objective BO to fine-tune the

processing conditions is expected to allow optimization of the copolymer composition together with adjustment of physical properties.

INTRODUCTION

Polymeric materials have a wide range of applications in both everyday life and specialized high-technology sectors, including in packaging, automotive engineering, medical devices and photonics. This ubiquity renders polymer science a critical aspect of industrial research. One of the key determinants of polymer properties is the monomer proportions. Specifically, achieving an optimal composition during copolymer synthesis is of paramount importance, as this factor directly affects attributes such as mechanical strength and thermal stability.[1–3] The relative reactivities of monomers are particularly significant and vary considerably, depending on the monomer combination that is used. This variability often leads to composition drift, a phenomenon where the actual monomer ratio in the copolymer deviates from the raw material ratio. Hence, this factor must be considered when designing a polymer synthesis to ensure that the synthesis process is robust against such deviations.[4–8] Moreover, the development of synthetic processes for homogeneous polymers having balanced monomer ratios, while accounting for the inevitability of composition drift, is crucial, both to ensure product

quality and to allow for scale-up to industrial production levels.

Historically, the exploration of new materials, including the design and process optimization stages, has been carried out primarily on an empirical basis, relying on iterative trial-and-error experimentation that consumes substantial time and resources. However, recent advancements in materials informatics, particularly machine learning, offer promising alternatives. As examples, machine learning techniques have been employed in composition searches,[9–13] crystal phase and microstructure classifications[14,15] and physical property predictions.[16,17] Within the field of polymer chemistry, informatics is increasingly being applied to the design of polymers[18–21] and the prediction of properties[22–24] based on the use of molecular descriptors. Bayesian optimization (BO), in particular, has emerged as a powerful tool in many scientific disciplines, including materials science.[25–29] This technique constructs a mathematical model using existing data and employs an acquisition function to quantitatively select experimental conditions for subsequent investigations. This data-driven approach obviates the need for experiential judgment and permits the identification of optimal conditions with fewer experimental iterations.[30] As an example, Nagato et al. successfully applied BO to the identification of processing conditions that minimized the formation of defects in powder films while carrying out a limited number of

experiments.[31]

Given that BO is predicated on the acquisition of experimental data, numerous experiments are typically required for method validation and so it is advantageous to employ experimental techniques capable of generating abundant, highly reproducible data. In this context, high-throughput methods for materials exploration[32–35] and analysis[36–38] are increasingly being integrated with machine learning algorithms.[39–41] Recent developments in microchemistry have led to the investigation of polymerization through flow synthesis, initially facilitated by micromixer-based systems.[42–47] Flow synthesis offers several benefits, including homogeneous mixing, efficient heat exchange, precise residence time control and scalability[48–50], making it a suitable candidate for integration with machine learning techniques.[51–57] Warren et al. previously developed a polymer synthesis and analysis platform that allowed RAFT polymerization to be automated and used this system to explore the trade-off between molar mass dispersity and monomer conversion[58]. In our previous work, we developed a flow copolymerization system based on a microflow mixer and explored the relationship between process conditions and reactivity ratios in styrene - methyl methacrylate (St-MMA) and glycidyl methacrylate - MMA copolymers.[59] This prior study also incorporated the prediction of physical properties when using unlearned molecules as

monomers (that is, molecular extrapolation prediction) based on the use of density functional theory calculations to model MMA-based copolymers.[60] The present research employed BO to identify the optimal conditions for synthesizing St-MMA copolymers with targeted compositions. The findings presented herein are expected to enhance the efficiency of polymer design and synthesis and also catalyze further innovations. Moreover, synergistic combinations of BO and flow copolymerization systems as demonstrated in this work are likely to have a wide range of applications in industrial settings.

METHODS

Polymer synthesis and characterization

A binary copolymer consisting of St and MMA was produced via a free radical process using the flow synthesis apparatus depicted in Figure 1. This apparatus was employed in our previous studies and has been demonstrated to be capable of reproducible and precise synthesis with little variation in polymer properties, meaning that it is suitable for generating data amenable to machine learning applications.[59,60] Various processing parameters (the proportion of St in the raw materials, the proportion of MMA, the amount of initiator, the solvent-to-monomer ratio (SM), the flow rate (which in turn,

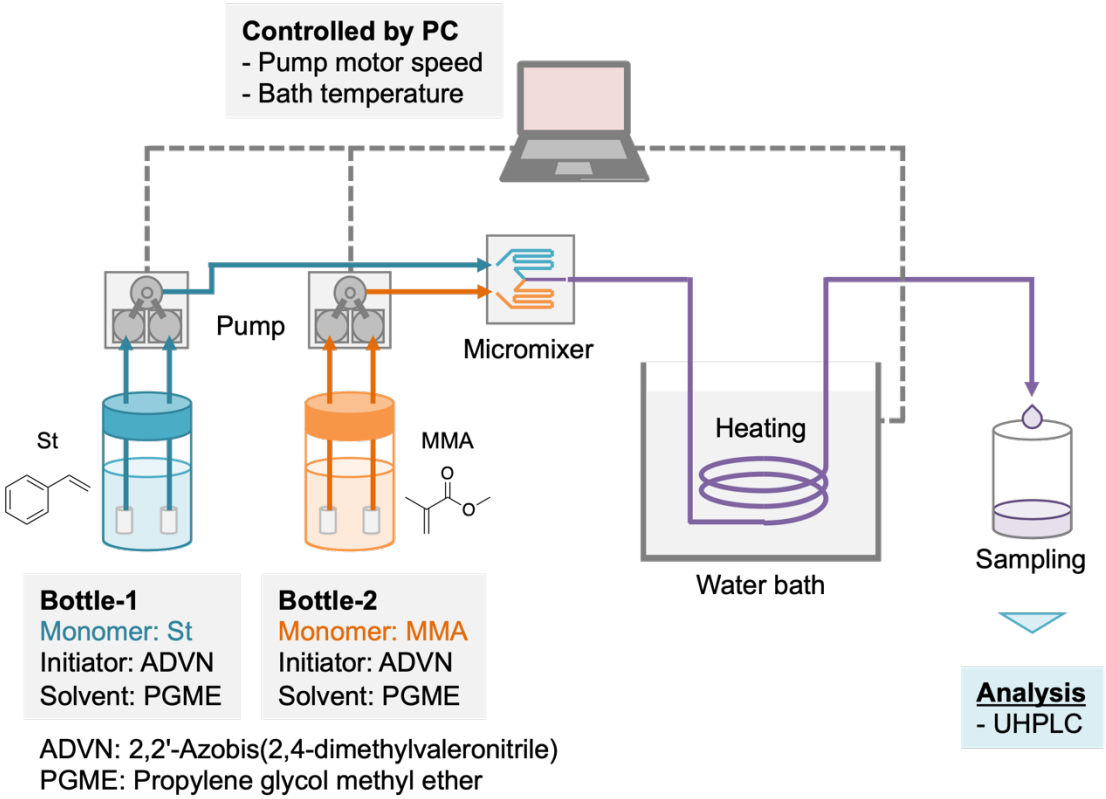

Figure 1. Diagram of the flow synthesis reactor. Streams from two bottles, each containing one monomer along with the initiator and solvent, were combined using a micromixer such that copolymers were synthesized at specific temperatures.

determined the reaction time) and the reaction temperature) were involved in the synthesis of individual copolymer specimens. During these trials, Bottle-1 contained the St, initiator and solvent while Bottle-2 held a mixture of MMA, initiator and solvent. The flow apparatus used in this work allowed the reaction time and monomer ratio to be readily adjusted by modifying the flow rates. However, it should be noted that the SM value and initiator proportion were determined during the preparation of the reagent mixture in each bottle and thus could not be changed merely by adjusting the flow rate.

Additionally, although the reaction temperature could be varied, this was not a simple process because some time was required for thermal equilibration with each change. Henceforth, the present work differentiates between easily adjustable process variables referred to as "soft process variables" (comprising the reaction time and monomer ratio) and less easily adjustable parameters referred to as "hard process variables" (that is, the SM value, initiator concentration and reaction temperature).

The copolymers synthesized in this work were analyzed using ultra-high-performance liquid chromatography (UHPLC) to determine the monomer polymerization percentages (M1 and M2) and the compositions of the copolymers. It should be noted that the UHPLC system was not integrated into the flow synthesis apparatus but rather was a separate analysis. These values were calculated as

$$St\ (or\ MMA)\ conv.(\%) = \left(1 - \frac{R_t}{R_0}\right) \times 100 \qquad (1)$$

and

$$St_{CR} = \frac{(St_{fr} \times St\ conv.)}{(St_{fr} \times St\ conv.) + (MMA_{fr} \times MMA\ conv.)} \times 100, \qquad (2)$$

where R_0 is the mass fraction of each monomer prior to the reaction, R_t is the mass fraction of each monomer at reaction time t, and St_{fr} and MMA_{fr} are the proportions of each monomer employed in the raw materials mixture in the synthetic procedure. To

assess the robustness of this analysis, multiple replicate analyses were performed to obtain the experimental error for monomer conversion in the form of a standard deviation, which was determined to be 0.19%. A total of 314 copolymers were synthesized using Latin hypercube sampling (LHS) and BO to determine the synthetic conditions. Details of the experimental and analytical conditions are provided in the Electronic Supplementary Information (ESI) for this paper.

Bayesian Optimization Algorithm

The BO method is a technique that can be used to efficiently explore explanatory variables that can be adjusted to minimize (or maximize) the output of an objective function, which is to be optimized.[61] In the present research, five process variables (the concentration of initiator, SM value, St proportion in the raw materials, reaction temperature and reaction time) were assessed as explanatory variables while the St proportion within the St-MMA copolymer was used as the objective outcome. Previous experiments[59] demonstrated that the monomer reactivity ratio can change depending on the synthesis conditions. This can occur even at an St concentration is 50%, which is close to the azeotropic boiling point of the St-MMA system. As a test case, the goal of the present study was to achieve an St proportion of 50 mol% within the copolymer. The

variable to be optimized to remove the effects of negative differences was defined as

$$y = (\text{Target St proportion in copolymer} - \text{Actual St proportion in copolymer})^2. \quad (3)$$

Since the target St proportion in the copolymer for this experiment was 50 mol%, the values of y ranged from 0 to 2500, with values closer to 0 indicating a composition closer to the target. A Matern 5/2 kernel was used to perform Gaussian regressions during these calculations. The Matern 5/2 covariance function was defined as

$$k(x, x') = \left(1 + \frac{\sqrt{5}r}{\theta} + \frac{5r^2}{3\theta^2}\right) exp\left(-\frac{\sqrt{5}r}{\theta}\right) \qquad (r = |x - x'|) \quad (4)$$

where θ is a scaling parameter. The Matern kernel is a smoothing function between the exponential kernel and RBF kernel, and was selected for use in this work because it was considered best suited to the analysis of the data.

The monomer reactivity values for St and MMA are 0.52 and 0.46, respectively.[62] It was unlikely that the monomer proportions in the St-MMA copolymers would deviate significantly from the nominal values due to the similar reactivity ratios for St and MMA as well as the target St proportion of 50 mol%. Therefore, this work focused solely on the St proportion in the copolymer. In addition, the difference between the St proportion in the initial monomer feed and that in the actual copolymer was assumed to be random and normally distributed. A 95% confidence interval for this

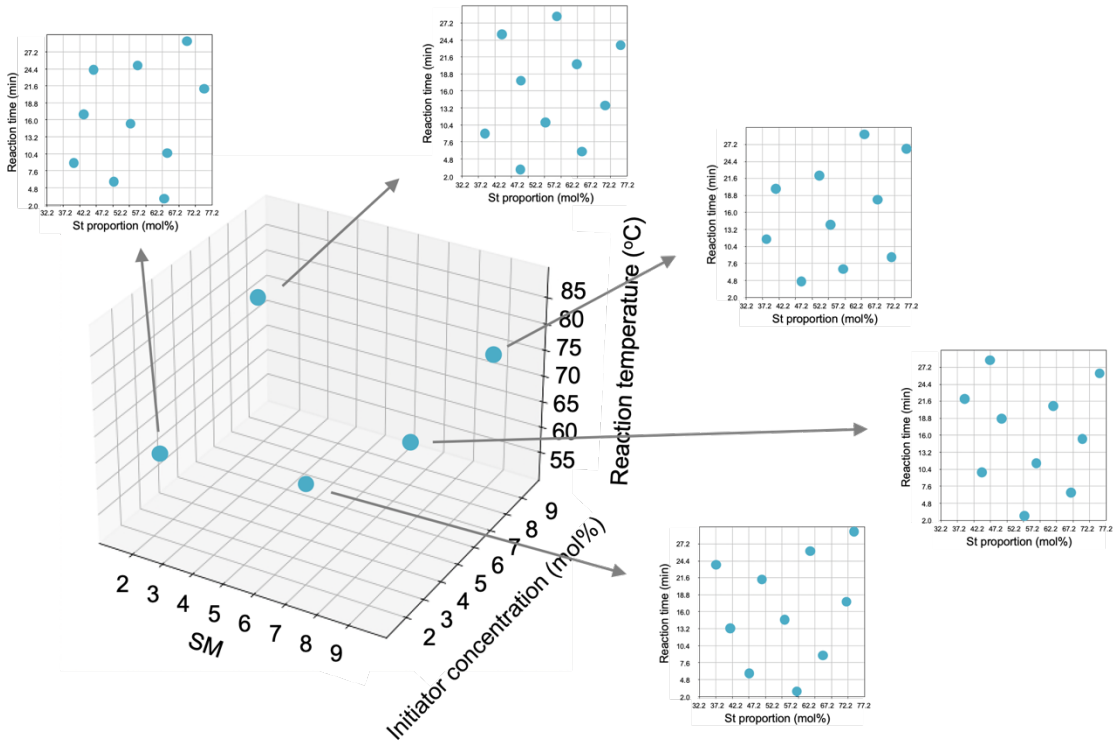

Figure 2. Plot of 50 initial points created using LHS. Initial point generation was performed with minimal bias within the search area. Following this, LHS was used to obtain five points in the hard process variable space then 10 points with changed values in the soft process variable space, for a total of 50 initial points.

variable was then calculated based on the standard deviation of the initial data (data obtained from 50 initial points, described below), and this interval was set as the search range for the St proportion (Table 1). Herein, the search range refers to the range of experimental conditions that BO may propose. BO was performed using the BoTorch Python library[63] while selecting Expected Improvement as the acquisition function. An LHS process was used for initial point sampling, obtaining 50 such points based on the maximin criterion. Figure 2 illustrates the initial point sampling method employed in

Table 1. BO ranges for the variables considered in this work.

Process variable	Range
Initiator concentration (mol%)	1 - 10
SM value	1 - 10
St proportion (mol%)	36.2 - 82.2
Reaction temperature (°C)	50 - 90
Reaction time (min)	2 - 30

Table 2. Initial point sampling ranges during LHS.

Process variable	Range
Initiator concentration (mol%)	1 - 10
SM value	1 - 10
St proportion (mol%)	0 - 100
Reaction temperature (°C)	50 - 90
Reaction time (min)	2 - 30

this study while the LHS search range is provided in Table 2. Because it was time-consuming to vary the so-called hard process variables, LHS was first carried out in the hard process variable space to obtain five points. Subsequently, based on these points, a further LHS was conducted in the soft process variable space to obtain 10 experimental conditions per hard process variable, resulting in a total of 50 initial points. Details concerning these initial points can be found in the ESI.

During the BO, certain processing conditions, such as the use of an overly low temperature, could possibly have resulted in incomplete copolymerization, leading to inaccurate assessments of copolymer properties. As such, these data points corresponded to missing values in the objective function. To address this, the present

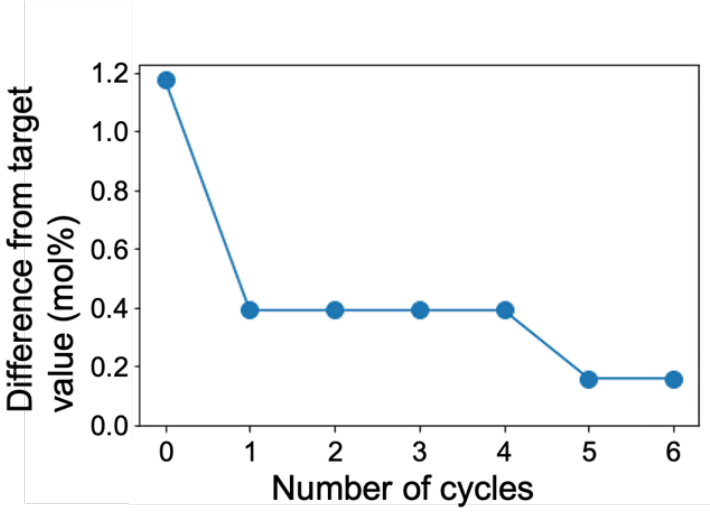

Figure 3. Minimum absolute value difference between target and experimental values for St proportion in copolymer for each cycle.

work adopted the so-called floor padding trick, which assigns the worst (herein y = 2500) experimental values to the missing values.[25]

RESULTS AND DISCUSSION

Bayesian optimization of monomer proportions in copolymers

This work employed BO with the goal of obtaining a 50 mole% St proportion in the copolymer. During this optimization, the model was updated every four candidate points and Figure 3 plots the minimum absolute difference between the target and experimental St proportions as a function of the number of optimization cycles. As described in the Methods section, the experimental error associated with these data was determined to be 0.19%. Consequently, an absolute difference of less than or equal to

Table 3. Process conditions associated with the optimum point, including explanatory variables and the St proportion in the copolymer during the optimization process.

		initial-15	candidate-1-1	candidate-5-3
Initiator concentration	(mol%)	8.195	8.950	10.00
SM value		1.186	6.420	8.120
St proportion	(mol%)	47.55	48.16	57.23
Reaction temperature	(°C)	73.40	69.20	67.54
Reaction time	(min)	13.99	18.98	27.06
St proportion in the copolymer	(mol%)	48.83	50.39	50.16

0.19% was considered to indicate that the desired copolymer composition had been attained. The optimization loop concluded after the fifth cycle, at which point the difference was 0.16% and therefore sufficiently small. Table 3 summarizes the ranges of process variable values employed in these trials and the monomer proportions achieved through the BO process. Herein, samples are named using the formula "initial-experiment condition no." for the initial points and "candidate-cycle no.-experiment condition no." for the BO results. As an example, "initial-15" describes the 15th experimental condition at the initial point while "candidate-5-3" describes the 3rd experimental condition in the 5th cycle of the BO process. The optimal initial point was initial-15, the optimal point from cycle 1 to cycle 4 was candidate-1-1, and the optimal point in cycle 5 was candidate-5-3, which was not updated in cycle 6.

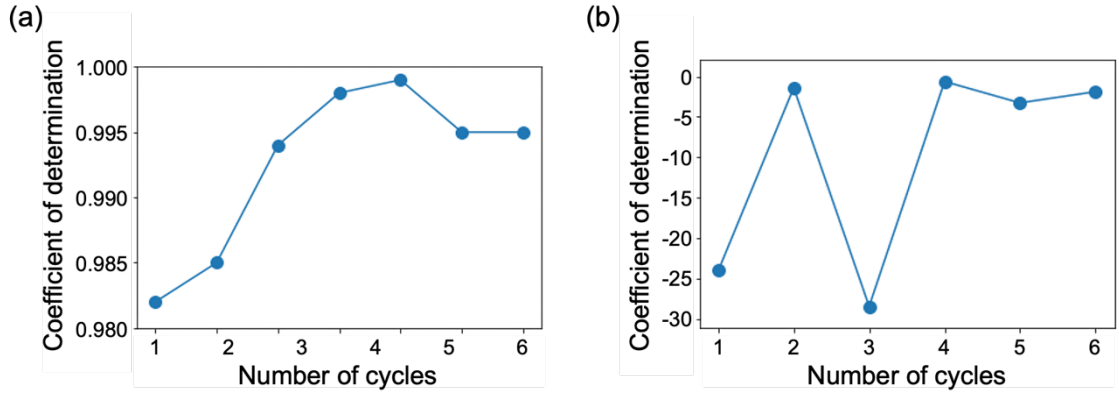

Figure 4. Predictive accuracies for (a) training data and (b) test data in each cycle. These plots show the shift in prediction accuracy as the BO progressed.

Throughout this optimization, numerous initial sampling points were employed that included a point close to the target (initial-15), although the St proportion in the copolymer remained below the desired value. Therefore, the St proportion is considered to have increased during the optimization process using the BO method. Furthermore, this process suggested a lower temperature, an extended reaction time and an increase in the SM value (that is, lowering the monomer concentration). These adjustments are discussed in detail in the following section. The results of this process also demonstrated that extending the reaction time was beneficial in the case that the St proportion was increased. The utility of lowering the reaction temperature was also apparent because the effects of decreasing the temperature and reducing the reaction time were typically opposite to one another.

The accuracy of the Gaussian regression performed for each optimization cycle was assessed by calculating the coefficient of determination using the existing training data and the flow synthesis results for the candidate points as test data (see Figures 4(a) and (b), respectively). While the predictive accuracy associated with the training data was found to be acceptable, the accuracy for the test data evidently improved with increases in the number of optimization cycles but remained low, with a coefficient of determination of -1.819 at the end of the optimization loop. This poor performance was attributed to a lack of sufficient experimental data extending over the entire search range, which affected the overall Gaussian regression. Even so, given that the primary aim of the present work was to achieve a specific copolymer composition, further improvements in the regression performance were not pursued.

Figure 5 plots the BO acquisition function values against the number of cycles. The acquisition function can be seen to have generally decreased as the optimization progressed, transitioning to a simple exploitation phase and increasingly proposing process conditions similar to those already tested. In this study, even though the acquisition function remained above zero, we were able to achieve the target copolymer composition. This outcome suggests that multiple sets of process conditions may have allowed this same goal to be accomplished. Additional optimization trials could

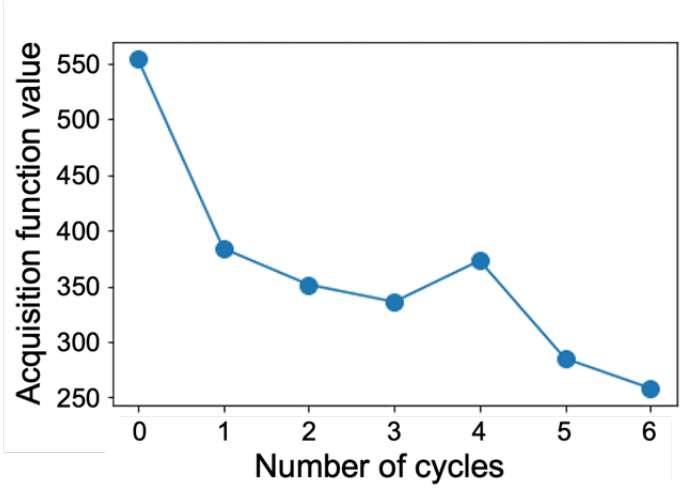

Figure 5. Acquisition function values versus the number of cycles.
These data indicate changes in the acquisition function as the BO progressed.

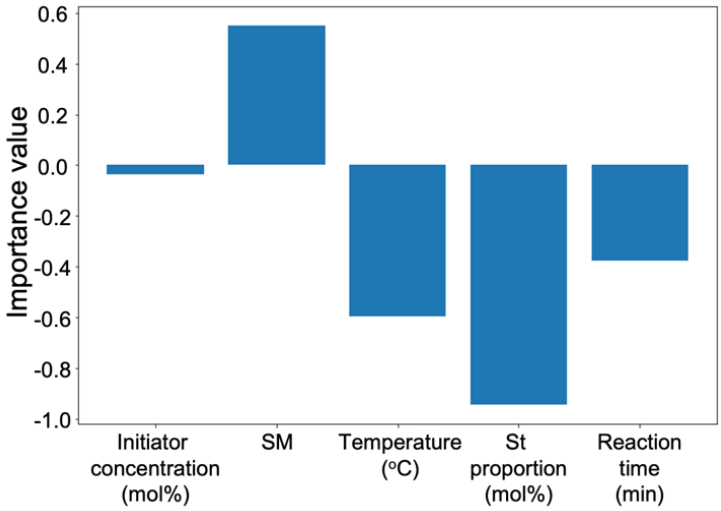

Figure 6. Importance value for each process variable using (target monomer proportion - experimental value)^2 as the objective variable.

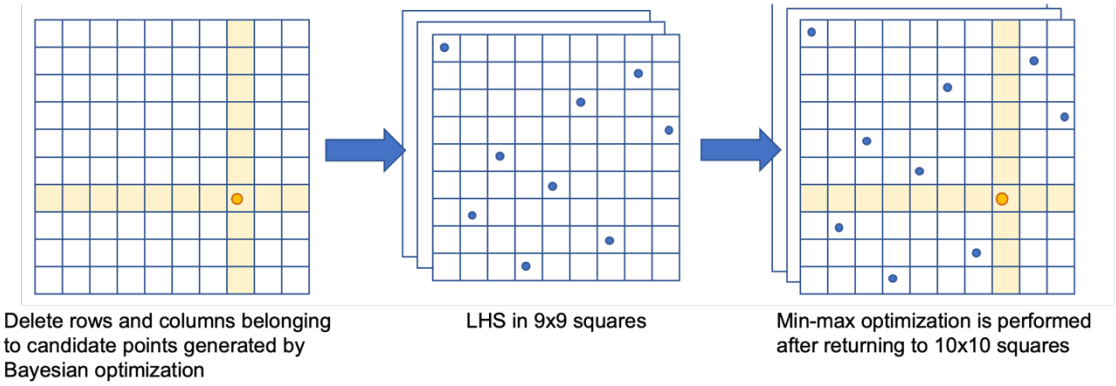

Figure 7. Diagram summarizing the method used to generate candidate points during extended BO. In this process, candidate points were extended using LHS while considering the points proposed by BO.

therefore potentially discover other feasible sets of process conditions, as addressed in more detail in the following section.

Finally, automatic relevance determination (ARD) was used to ascertain the importance of each process variable, as represented by the common logarithm of the length scale (Figure 6). The SM value was found to be the most important variable, whereas the St proportion was the least important. Typically, the desired composition of a copolymer is achieved by adjusting the monomer proportions in the raw material mixture, which are considered important factors in experimental work. The low importance of the St proportion in the present work can be attributed to the fact that all five process variables affected the copolymer composition and that the search range included experimental conditions that did not promote radical polymerization. Because the St proportion had a minimal effect with regard to whether the polymerization

reaction proceeded, the relative importance of this variable was found to be low. This result demonstrates that machine learning can explicitly reveal what humans may implicitly taken for granted. Additional trials are currently underway in our laboratory to assess the apparent high importance of the SM value, which may be related to solvent effects, using molecular dynamics simulations. The results will be reported in a separate paper.

Extended Bayesian optimization of monomer proportions in the copolymer

The results described in the previous section based on BO during which the function was updated every four candidate points suggested that multiple sets of conditions could potentially give the target copolymer composition. To assess this possibility, an extended BO (EBO) was performed using the same flow apparatus but updating the function every 40 candidate points. These 40 points included four points output by the original BO and an additional 36 points generated using LHS for the continuously varied soft process variables (monomer proportions and reaction time) (Figure 7).

Firstly, a comparison between the EBO and BO results was conducted. Figure 8 plots changes in the minimum absolute difference between the target and experimental St proportions versus the number of optimization loop cycles. Contrary to expectations,

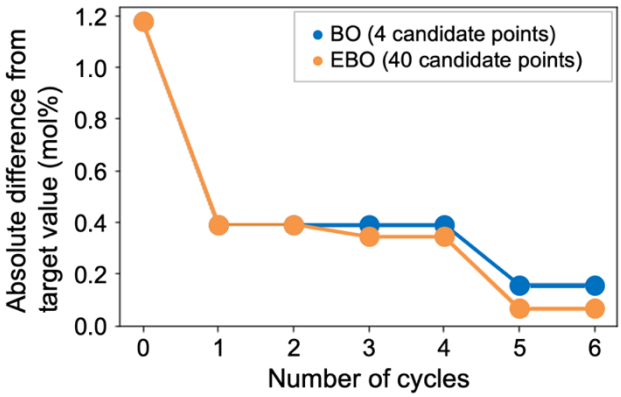

Figure 8. Smallest absolute differences between target and experimental values as functions of the number of cycles for four and 40 candidates points.

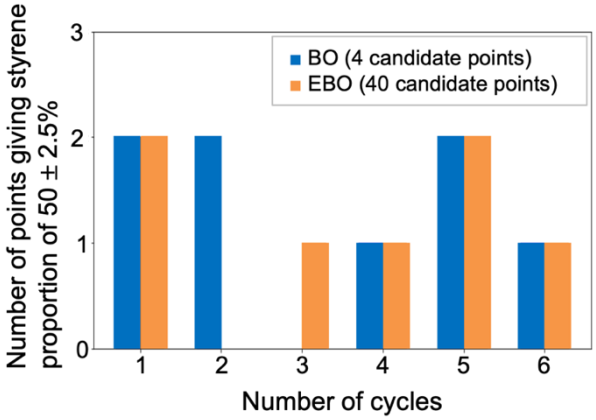

Figure 9. Number of conditions for which the monomer proportion in the copolymer was 50 ± 2.5 mol% among candidate points generated by BO for various numbers of cycles.

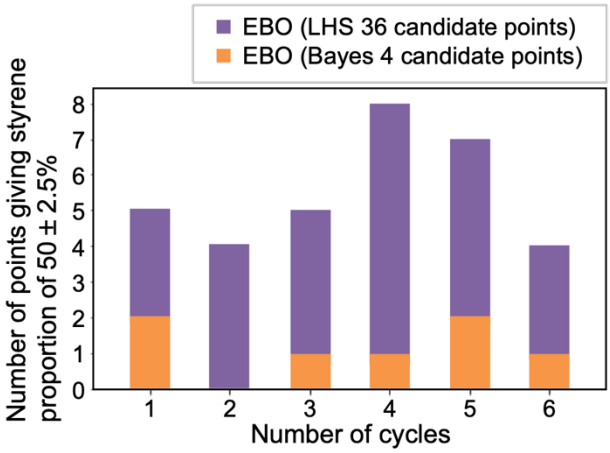

Figure 10. Comparison of the number of experimental conditions achieving the target value (St proportion of 50 ± 2.5 mol%) using the Bayesian approach and LHS.

no significant change was observed in either the number of cycles required for optimization or the minimum absolute difference between the target and experimental values at each cycle. Figure 9 summarizes the number of data points that achieved an St proportion within the copolymer of 50±2.5% from the four candidate points generated in each cycle for both the BO and EBO. A span of ±2.5% was employed here based on the range that would be considered acceptable for commercial products. After six cycles of BO, eight and seven samples, respectively, achieved the desired composition in association with BO and EBO. Hence, no significant advantage was obtained from the expanded set of candidate points. Possible reasons for these results include the use of a sufficient number of initial data points and the low importance of the extended conditions (that is, the St proportion in the raw materials and the reaction time), as shown in Figure 6. While it would have been beneficial to increase the number of samples meeting the required criteria in the four candidate points predicted by the Bayesian optimization of the EBO method, this was not achieved in the present study. Because the EBO method allowed ten different conditions of experimental conditions to be examined per day (compared with only one or two combinations per day when using the BO technique), more experiments could be performed in a given time frame and at a lower cost, resulting in a larger quantity of samples meeting the required criteria. For

this reason, the EBO method was employed in the present research.

Figure 10 presents the number of data points required to obtain an St proportion in the copolymer of 50 ± 2.5% at each cycle for all 240 candidate points, including the extended points obtained through EBO. Following six EBO cycles, 33 conditions that provided the desired composition were discovered. Although many suitable sets of conditions were identified in the extended region, the probability of discovery was higher in the case of the candidate points resulting from the BO process. This likely occurred because the extended process variables were determined by LHS and thus were not intended to achieve the target composition. Despite this, suitable conditions were found, possibly as a consequence of the relatively high importance of the three hard process variables proposed by the BO.

The predictive distribution generated by the Gaussian regression up to the sixth optimization cycle was visualized using partial dependent plots (PDPs)[64] to display the relationships between groups of two process variables and the target variable (Figure 11). In these plots, the color represents the predictive mean value obtained from Gaussian regression, with shades closer to blue indicating proximity to the target composition. As such, plots exhibiting a large blue area suggest that multiple conditions could achieve the desired composition. As an example, Figure 11(e) shows the

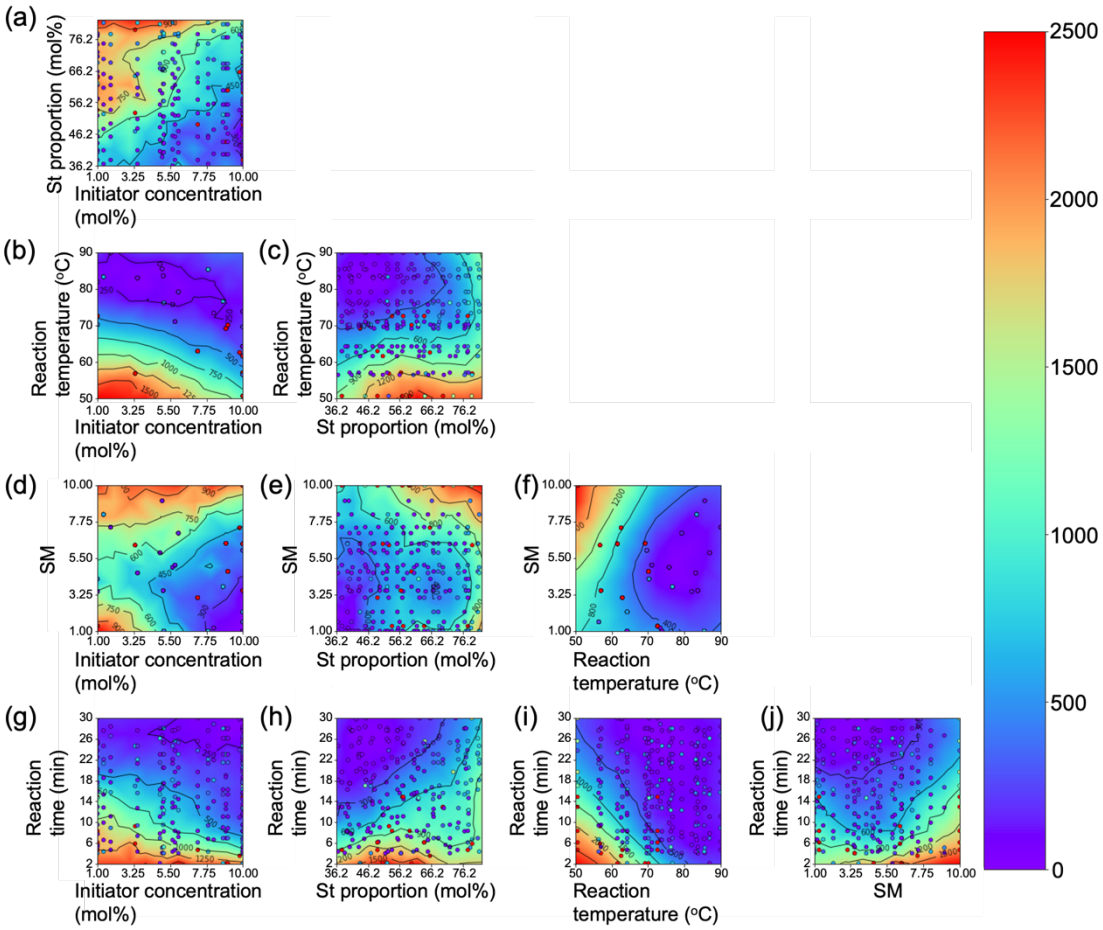

Figure 11. PDP diagrams showing the predicted mean of the sixth optimized Gaussian process regression obtained using EBO for each pair of explanatory variables. The color-coded numerical values are the predicted means of the Gaussian regression, with colors closer to blue corresponding to values closer to the target proportion.

relationship between the SM value and the St proportion. Here, two blue regions are evident, within which the St proportion occupies a large region around 40% and a smaller region around 65%. This observation implies the existence of multiple trends in the variable combinations conducive to reaching the ideal 50% monomer proportion. Moreover, in Figure 11(h) the blue regions are predominantly situated in the upper left quadrant, indicating the advantage of extending the reaction time when increasing the St proportion, as previously discussed in relation to the BO. Similarly, Figure 11 (i) demonstrates that as the reaction temperature increases, the range of reaction times over which the target value is achieved expands. This finding provides further evidence that a simplistic optimization approach targeting a 50% monomer composition is insufficient.

To further validate these findings, clustering was performed in the space of the five process variables for the 35 data points that achieved an St proportion in the copolymer of 50 ± 2.5%. These analyses used k-means and were visualized based on principal coordinate analysis (PCA) and parallel plots (Figures 12 and 13). Four clusters were classified and color-coded, and the color-coding in the PCA and parallel plots correspond to one another. The parallel plots establish that Cluster 1 was associated with conditions for which the St proportion was above 50% whereas Clusters 2 and 3 had proportions below 50%. Cluster 4, considered an outlier, had only two conditions (for

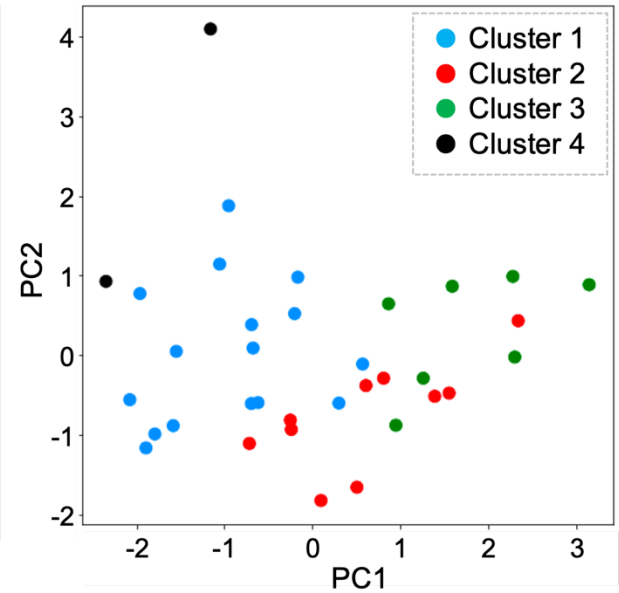

Figure 12. PCA results obtained from data related to achieving 50 ± 2.5 mol% St proportion in copolymer.

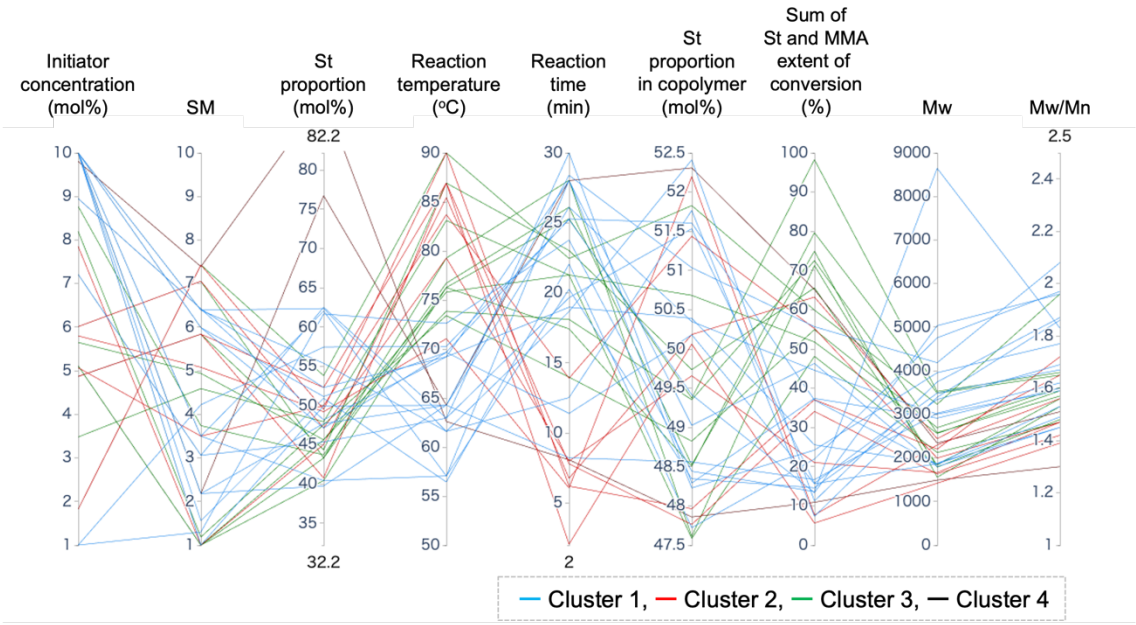

Figure 13. Processing conditions related to achieving 50 ± 2.5 mol% St proportion in the copolymer. Each cluster is illustrated in a different color. Explanatory variables, objective variables and other important physical properties (sum of St and MMA conversion percentages, Mw and Mw/Mn) are indicated in each case that the desired St proportion is achieved.

which the St proportions were above 70%). When comparing parameters other than the St proportion, it can be seen that Cluster 1 involved high initiator amounts, low SM values, low reaction temperatures and long reaction times, while Cluster 2 had moderate initiator amounts, high SM values, high reaction temperatures and short reaction times. Cluster 3 involved conditions that were intermediate between those of Clusters 1 and 2. In addition, Cluster 1 was associated with high Mw and Mw/Mn values while Cluster 2 showed low Mw and Mw/Mn values. These results can be ascribed to the temperature-dependent initiation mechanism that, in turn, affected the copolymer chain lengths. Specifically, at lower temperatures (as is evident from the Cluster 1 data), initiator cleavage would occur sporadically, leading to a gradual increase in polymerization initiation points and the formation of heterogeneous, high-molecular-weight molecules. In contrast, at the elevated temperatures typified by Cluster 2, the initiator molecules would be expected to undergo simultaneous cleavage to give shorter chains.

In summary, the single-task BO revealed multiple process conditions and trends that were capable of providing the target copolymer composition. Furthermore, as shown in Figure 13, parameters other than the copolymer composition, such as the extent of monomer conversion, Mw and Mw/Mn, varied significantly depending on the process conditions. These parameters would likely affect the copolymer characteristics

and so should also be optimized in a real-world scenario. This process would correspond to a so-called multi-objective BO and has been previously applied to the design of various materials and been shown to be effective.[65–69] We propose that the aforementioned challenges could be addressed through empirical validation using multi-objective BO.

CONCLUSIONS

This study elucidated the process conditions required to optimize the monomer proportions in a copolymer through the use of BO in conjunction with a flow synthesis apparatus. Notably, the solvent concentration was found to be more critical than the monomer proportions in the raw materials. This finding is corroborated by our previous research, which demonstrated that relative reactivities of monomers can change depending on the process conditions. Hence, this work is expected to lead to further mechanistic elucidation from a molecular perspective. The use of EBO also revealed that numerous sets of conditions could give the desired copolymer composition. A comparison of these conditions established multiple trends and provided insights into the radical polymerization mechanism. Even in the case that the target composition was achieved, other polymer properties (specifically the extent of monomer conversion, Mw

and Mw/Mn) varied significantly. These properties have a direct impact on the physical properties of a polymer and thus should be optimized concurrently. Future work by our group will involve verification using multi-objective BO to address these challenges, which is expected to eventually lead to practical applications. Ultimately, our goal is to control polymer properties using these optimization techniques so as to create new value through scalable development and manufacturing.

Author Contributions

S. Takasuka: Investigation (EXP), Writing - Original Draft. S. Ito: Investigation (ML, EXP). S. Oikawa: Software. Y. Harashima: Resources. T. Takayama: Formal analysis (EXP). Aniruddha Nag: Investigation (EXP). Araki Wakiuchi: Investigation (EXP), Software. T. Ando: Formal analysis (EXP), T. Sugawara: Conceptualization (EXP), Formal analysis (EXP). M. Hatanaka: Formal analysis (ML). T. Miyao: Formal analysis (ML). T. Matsubara: Supervision (ML). Y. Ohnishi: Formal analysis (ML). H. Ajiro: Investigation (EXP). M. Fujii: Project administration. Legend: ML and EXP represent machine learning and experiments.s

Conflicts of interest

The authors declare no competing financial interest.

Acknowledgments

This article is based on results obtained from a project (no. JPNP14004) funded by the New Energy and Industrial Technology Development Organization (NEDO), Japan, and by a Japan Society for the Promotion of Science (JSPS) KAKENHI grant (no. JP21K20537).

REFERENCES

(1) Terao, Y.; Sugihara, S.; Satoh, K.; Kamigaito, M. 1:3 ABAA Sequence-Regulated Substituted Polymethylenes via Alternating Radical Copolymerization of Methyl Cinnamate and Maleic Anhydride Followed by Post-Polymerization Reactions. *Eur. Polym. J.* **2019**, *120*, 109225. https://doi.org/10.1016/j.eurpolymj.2019.109225.

(2) Shibata, M.; Sugane, K.; Yanagisawa, Y. Biobased Polymer Networks by the Thiol-Ene Photopolymerization of Allylated p-Coumaric and Caffeic Acids. *Polym. J.* **2019**, *51* (5), 461–470. https://doi.org/10.1038/s41428-018-0165-0.

(3) Takasuka, S.; Takahashi, K.; Takahashi, T. Characterization and Mechanical

Strength of Wholly Aromatic Liquid Crystalline Polymers with Low Melting Point. *Int. J. Polym. Anal. Charact.* **2022**, *27* (1), 43–51. https://doi.org/10.1080/1023666X.2021.2004012.

(4) Kotani, Y.; Kamigaito, M.; Sawamoto, M. Living Random Copolymerization of Styrene and Methyl Methacrylate with a Ru(II) Complex and Synthesis of ABC-Type "Block-Random" Copolymers. *Macromolecules* **1998**, *31* (17), 5582–5587. https://doi.org/10.1021/ma980294x.

(5) Schweer, J. Penultimate Model Description of the Propagation Kinetics for the Free Radical Copolymerization of Styrene and Methyl Methacrylate. *Makromol. Chem. Theory Simul.* **1993**, *2* (3), 485–502. https://doi.org/10.1002/mats.1993.040020313.

(6) Ishizu, K.; Park, J.; Ohta, Y.; Shibuya, T. Synthesis and Characterization of Methyl Methacrylate/Styrene Hyperbranched Copolymers via Living Radical Mechanism. *J. Appl. Polym. Sci.* **2003**, *89* (9), 2490–2495. https://doi.org/10.1002/app.12161.

(7) Neugebauer, D.; Bury, K.; Wlazło, M. Atom Transfer Radical Copolymerization of Glycidyl Methacrylate and Methyl Methacrylate. *J. Appl. Polym. Sci.* **2012**, *124* (3), 2209–2215. https://doi.org/10.1002/app.35234.

(8) Reddy, B. S. R.; Balasubramanian, S. Novel Activated Acrylates: Synthesis,

Characterization and the Reactivity Ratios of 4-Acetamidophenyl Acrylate Copolymers with Methyl Methacrylate and Glycidyl Methacrylate. *Eur. Polym. J.* **2002**, *38* (4), 803–813. https://doi.org/10.1016/S0014-3057(01)00242-7.

(9) Trehern, W.; Ortiz-Ayala, R.; Atli, K. C.; Arroyave, R.; Karaman, I. Data-Driven Shape Memory Alloy Discovery Using Artificial Intelligence Materials Selection (AIMS) Framework. *Acta Mater.* **2022**, *228*, 117751. https://doi.org/10.1016/j.actamat.2022.117751.

(10) Shafe, A.; Wick, C. D.; Peters, A. J.; Liu, X.; Li, G. Effect of Atomistic Fingerprints on Thermomechanical Properties of Epoxy-Diamine Thermoset Shape Memory Polymers. *Polymer* **2022**, *242*, 124577. https://doi.org/10.1016/j.polymer.2022.124577.

(11) Ihalage, A.; Hao, Y. Formula Graph Self-Attention Network for Representation-Domain Independent Materials Discovery. *Adv. Sci.* **2022**, *9* (18), 2200164. https://doi.org/10.1002/advs.202200164.

(12) Ma, R.; Zhang, H.; Luo, T. Exploring High Thermal Conductivity Amorphous Polymers Using Reinforcement Learning. *ACS Appl. Mater. Interfaces* **2022**, *14* (13), 15587–15598. https://doi.org/10.1021/acsami.1c23610.

(13) Kuenneth, C.; Schertzer, W.; Ramprasad, R. Copolymer Informatics with

Multitask Deep Neural Networks. *Macromolecules* **2021**, *54* (13), 5957–5961. https://doi.org/10.1021/acs.macromol.1c00728.

(14) Mishra, S. P.; Rahul, M. R. A Comparative Study and Development of a Novel Deep Learning Architecture for Accelerated Identification of Microstructure in Materials Science. *Comput. Mater. Sci.* **2021**, *200*, 110815. https://doi.org/10.1016/j.commatsci.2021.110815.

(15) Machaka, R. Machine Learning-Based Prediction of Phases in High-Entropy Alloys. *Comput. Mater. Sci.* **2021**, *188*, 110244. https://doi.org/10.1016/j.commatsci.2020.110244.

(16) Pugar, J. A.; Gang, C.; Huang, C.; Haider, K. W.; Washburn, N. R. Predicting Young's Modulus of Linear Polyurethane and Polyurethane–Polyurea Elastomers: Bridging Length Scales with Physicochemical Modeling and Machine Learning. *ACS Appl. Mater. Interfaces* **2022**, *14* (14), 16568–16581. https://doi.org/10.1021/acsami.1c24715.

(17) Patra, A.; Batra, R.; Chandrasekaran, A.; Kim, C.; Huan, T. D.; Ramprasad, R. A Multi-Fidelity Information-Fusion Approach to Machine Learn and Predict Polymer Bandgap. *Comput. Mater. Sci.* **2020**, *172*, 109286. https://doi.org/10.1016/j.commatsci.2019.109286.

(18) Aldeghi, M.; Coley, C. W. A Graph Representation of Molecular Ensembles for Polymer Property Prediction. *Chem. Sci.* **2022**, *13* (35), 10486–10498. https://doi.org/10.1039/D2SC02839E.

(19) Liu, A. L.; Venkatesh, R.; McBride, M.; Reichmanis, E.; Meredith, J. C.; Grover, M. A. Small Data Machine Learning: Classification and Prediction of Poly(Ethylene Terephthalate) Stabilizers Using Molecular Descriptors. *ACS Appl. Polym. Mater.* **2020**, *2* (12), 5592–5601. https://doi.org/10.1021/acsapm.0c00921.

(20) Venkatraman, V.; Alsberg, B. Designing High-Refractive Index Polymers Using Materials Informatics. *Polymers* **2018**, *10* (1), 103. https://doi.org/10.3390/polym10010103.

(21) Tao, L.; Varshney, V.; Li, Y. Benchmarking Machine Learning Models for Polymer Informatics: An Example of Glass Transition Temperature. *J. Chem. Inf. Model.* **2021**, *61* (11), 5395–5413. https://doi.org/10.1021/acs.jcim.1c01031.

(22) Cravero, F.; Díaz, M. F.; Ponzoni, I. Polymer Informatics for QSPR Prediction of Tensile Mechanical Properties. Case Study: Strength at Break. *J. Chem. Phys.* **2022**, *156* (20), 204903. https://doi.org/10.1063/5.0087392.

(23) Kuenneth, C.; Rajan, A. C.; Tran, H.; Chen, L.; Kim, C.; Ramprasad, R. Polymer Informatics with Multi-Task Learning. *Patterns* **2021**, *2* (4), 100238.

https://doi.org/10.1016/j.patter.2021.100238.

(24) Park, J.; Shim, Y.; Lee, F.; Rammohan, A.; Goyal, S.; Shim, M.; Jeong, C.; Kim, D. S. Prediction and Interpretation of Polymer Properties Using the Graph Convolutional Network. *ACS Polym. Au* **2022**, *2* (4), 213–222. https://doi.org/10.1021/acspolymersau.1c00050.

(25) Wakabayashi, Y. K.; Otsuka, T.; Krockenberger, Y.; Sawada, H.; Taniyasu, Y.; Yamamoto, H. Bayesian Optimization with Experimental Failure for High-Throughput Materials Growth. *Npj Comput. Mater.* **2022**, *8* (1), 180. https://doi.org/10.1038/s41524-022-00859-8.

(26) Hanaoka, K. Bayesian Optimization for Goal-Oriented Multi-Objective Inverse Material Design. *iScience* **2021**, *24* (7), 102781. https://doi.org/10.1016/j.isci.2021.102781.

(27) Hughes, Z. E.; Nguyen, M. A.; Wang, J.; Liu, Y.; Swihart, M. T.; Poloczek, M.; Frazier, P. I.; Knecht, M. R.; Walsh, T. R. Tuning Materials-Binding Peptide Sequences toward Gold- and Silver-Binding Selectivity with Bayesian Optimization. *ACS Nano* **2021**, *15* (11), 18260–18269. https://doi.org/10.1021/acsnano.1c07298.

(28) Honarmandi, P.; Attari, V.; Arroyave, R. Accelerated Materials Design Using Batch Bayesian Optimization: A Case Study for Solving the Inverse Problem from

Materials Microstructure to Process Specification. *Comput. Mater. Sci.* **2022**, *210*, 111417. https://doi.org/10.1016/j.commatsci.2022.111417.

(29) Hooker, J.; Kovoor, J.; Jones, K. L.; Kanungo, R.; Alcorta, M.; Allen, J.; Andreoiu, C.; Atar, L.; Bardayan, D. W.; Bhattacharjee, S. S.; Blankstein, D.; Burbadge, C.; Burcher, S.; Catford, W. N.; Cha, S.; Chae, K.; Connolly, D.; Davids, B.; Esker, N.; Garcia, F. H.; Gillespie, S.; Ghimire, R.; Gula, A.; Hackman, G.; Hallam, S.; Hellmich, M.; Henderson, J.; Holl, M.; Jassal, P.; King, S.; Knight, T.; Kruecken, R.; Lepailleur, A.; Liang, J.; Morrison, L.; O'Malley, P. D.; Pain, S. D.; Pereira-Lopez, X.; Psaltis, A.; Radich, A.; Shotter, A. C.; Vostinar, M.; Williams, M.; Workman, O. Use of Bayesian Optimization to Understand the Structure of Nuclei. *Nucl. Instrum. Methods Phys. Res. Sect. B Beam Interact. Mater. At.* **2022**, *512*, 6–11. https://doi.org/10.1016/j.nimb.2021.11.014.

(30) Shahriari, B.; Swersky, K.; Wang, Z.; Adams, R. P.; De Freitas, N. Taking the Human Out of the Loop: A Review of Bayesian Optimization. *Proc. IEEE* **2016**, *104* (1), 148–175. https://doi.org/10.1109/JPROC.2015.2494218.

(31) Nagai, K.; Osa, T.; Inoue, G.; Tsujiguchi, T.; Araki, T.; Kuroda, Y.; Tomizawa, M.; Nagato, K. Sample-Efficient Parameter Exploration of the Powder Film Drying Process Using Experiment-Based Bayesian Optimization. *Sci. Rep.* **2022**, *12* (1), 1615.

https://doi.org/10.1038/s41598-022-05784-w.

(32) Santacruz, D.; Enane, F. O.; Fundel-Clemens, K.; Giner, M.; Wolf, G.; Onstein, S.; Klimek, C.; Smith, Z.; Wijayawardena, B.; Viollet, C. Automation of High-Throughput mRNA-Seq Library Preparation: A Robust, Hands-Free and Time Efficient Methodology. *SLAS Discov.* **2022**, *27* (2), 140–147. https://doi.org/10.1016/j.slasd.2022.01.002.

(33) Nandiwale, K. Y.; Hart, T.; Zahrt, A. F.; Nambiar, A. M. K.; Mahesh, P. T.; Mo, Y.; Nieves-Remacha, M. J.; Johnson, M. D.; García-Losada, P.; Mateos, C.; Rincón, J. A.; Jensen, K. F. Continuous Stirred-Tank Reactor Cascade Platform for Self-Optimization of Reactions Involving Solids. *React. Chem. Eng.* **2022**, *7* (6), 1315–1327. https://doi.org/10.1039/D2RE00054G.

(34) Brocken, L.; Price, P. D.; Whittaker, J.; Baxendale, I. R. Continuous Flow Synthesis of Poly(Acrylic Acid) via Free Radical Polymerisation. *React. Chem. Eng.* **2017**, *2* (5), 662–668. https://doi.org/10.1039/C7RE00063D.

(35) García-Lacuna, J.; Baumann, M. Inline Purification in Continuous Flow Synthesis – Opportunities and Challenges. *Beilstein J. Org. Chem.* **2022**, *18*, 1720–1740. https://doi.org/10.3762/bjoc.18.182.

(36) Yang, L.; Haber, J. A.; Armstrong, Z.; Yang, S. J.; Kan, K.; Zhou, L.; Richter,

M. H.; Roat, C.; Wagner, N.; Coram, M.; Berndl, M.; Riley, P.; Gregoire, J. M. Discovery of Complex Oxides via Automated Experiments and Data Science. *Proc. Natl. Acad. Sci.* **2021**, *118* (37), e2106042118. https://doi.org/10.1073/pnas.2106042118.

(37) Losacco, G. L.; Wang, H.; Haidar Ahmad, I. A.; DaSilva, J.; Makarov, A. A.; Mangion, I.; Gasparrini, F.; Lämmerhofer, M.; Armstrong, D. W.; Regalado, E. L. Enantioselective UHPLC Screening Combined with *In Silico* Modeling for Streamlined Development of Ultrafast Enantiopurity Assays. *Anal. Chem.* **2022**, *94* (3), 1804–1812. https://doi.org/10.1021/acs.analchem.1c04585.

(38) Bennett, R.; Cohen, R. D.; Wang, H.; Pereira, T.; Haverick, M. A.; Loughney, J. W.; Barbacci, D. C.; Pristatsky, P.; Bowman, A. M.; Losacco, G. L.; Richardson, D. D.; Mangion, I.; Regalado, E. L. Selective Plate-Based Assay for Trace EDTA Analysis via Boron Trifluoride-Methanol Derivatization UHPLC-QqQ-MS/MS Enabling Biologic and Vaccine Processes. *Anal. Chem.* **2022**, *94* (3), 1678–1685. https://doi.org/10.1021/acs.analchem.1c04224.

(39) Nambiar, A. M. K.; Breen, C. P.; Hart, T.; Kulesza, T.; Jamison, T. F.; Jensen, K. F. Bayesian Optimization of Computer-Proposed Multistep Synthetic Routes on an Automated Robotic Flow Platform. *ACS Cent. Sci.* **2022**, *8* (6), 825–836. https://doi.org/10.1021/acscentsci.2c00207.

(40) Kumar, R. Materiomically Designed Polymeric Vehicles for Nucleic Acids: Quo Vadis? *ACS Appl. Bio Mater.* **2022**, *5* (6), 2507–2535. https://doi.org/10.1021/acsabm.2c00346.

(41) Iwama, R.; Kaneko, H. Integration of Materials and Process Informatics: Metal Oxide and Process Design for CO_2 Reduction. *ACS Omega* **2022**, *7* (50), 46922–46934. https://doi.org/10.1021/acsomega.2c06008.

(42) Corrigan, N.; Almasri, A.; Taillades, W.; Xu, J.; Boyer, C. Controlling Molecular Weight Distributions through Photoinduced Flow Polymerization. *Macromolecules* **2017**, *50* (21), 8438–8448. https://doi.org/10.1021/acs.macromol.7b01890.

(43) Zhou, Y.; Gu, Y.; Jiang, K.; Chen, M. Droplet-Flow Photopolymerization Aided by Computer: Overcoming the Challenges of Viscosity and Facilitating the Generation of Copolymer Libraries. *Macromolecules* **2019**, *52* (15), 5611–5617. https://doi.org/10.1021/acs.macromol.9b00846.

(44) Wang, Z.; Zhou, Y.; Chen, M. Computer-aided Living Polymerization Conducted under Continuous-flow Conditions. *Chin. J. Chem.* **2022**, *40* (2), 285–296. https://doi.org/10.1002/cjoc.202100544.

(45) Zhang, B.; Mathoor, A.; Junkers, T. High Throughput Multidimensional

Kinetic Screening in Continuous Flow Reactors. *Angew. Chem. Int. Ed.* **2023**, *62* (38), e202308838. https://doi.org/10.1002/anie.202308838.

(46) Rubens, M.; Vrijsen, J. H.; Laun, J.; Junkers, T. Precise Polymer Synthesis by Autonomous Self-Optimizing Flow Reactors. *Angew. Chem. Int. Ed.* **2019**, *58* (10), 3183–3187. https://doi.org/10.1002/anie.201810384.

(47) Reis, M. H.; Leibfarth, F. A.; Pitet, L. M. Polymerizations in Continuous Flow: Recent Advances in the Synthesis of Diverse Polymeric Materials. *ACS Macro Lett.* **2020**, *9* (1), 123–133. https://doi.org/10.1021/acsmacrolett.9b00933.

(48) Knox, S. T.; Parkinson, S.; Stone, R.; Warren, N. J. Benchtop Flow-NMR for Rapid Online Monitoring of RAFT and Free Radical Polymerisation in Batch and Continuous Reactors. *Polym. Chem.* **2019**, *10* (35), 4774–4778. https://doi.org/10.1039/C9PY00982E.

(49) Zaquen, N.; Rubens, M.; Corrigan, N.; Xu, J.; Zetterlund, P. B.; Boyer, C.; Junkers, T. Polymer Synthesis in Continuous Flow Reactors. *Prog. Polym. Sci.* **2020**, *107*, 101256. https://doi.org/10.1016/j.progpolymsci.2020.101256.

(50) Walsh, D. J.; Schinski, D. A.; Schneider, R. A.; Guironnet, D. General Route to Design Polymer Molecular Weight Distributions through Flow Chemistry. *Nat. Commun.* **2020**, *11* (1), 3094. https://doi.org/10.1038/s41467-020-16874-6.

(51) Reis, M.; Gusev, F.; Taylor, N. G.; Chung, S. H.; Verber, M. D.; Lee, Y. Z.; Isayev, O.; Leibfarth, F. A. Machine-Learning-Guided Discovery of ^{19}F MRI Agents Enabled by Automated Copolymer Synthesis. *J. Am. Chem. Soc.* **2021**, *143* (42), 17677–17689. https://doi.org/10.1021/jacs.1c08181.

(52) Tan, J. D.; Ramalingam, B.; Wong, S. L.; Cheng, J.; Lim, Y.-F.; Chellappan, V.; Khan, S. A.; Kumar, J.; Hippalgaonkar, K. *Machine Learning Predicts Conversion and Molecular Weight Distributions in Computer Controlled Polymerization*; preprint; Chemistry, **2022**. https://doi.org/10.26434/chemrxiv-2022-tlz53.

(53) Gu, Y.; Lin, P.; Zhou, C.; Chen, M. Machine Learning-Assisted Systematical Polymerization Planning: Case Studies on Reversible-Deactivation Radical Polymerization. **2021***, 64*, 1039–1046. https://doi.org/10.1007/s11426-020-9969-y.

(54) Zhao, B.; Cheng, J.; Gao, J.; Haddleton, David. M.; Wilson, P. Active Learning as a Tool for Optimizing “Plug-n-Play” Electrochemical Atom Transfer Radical Polymerization. *Macromol. Chem. Phys.* **2023**, *224* (12), 2300039. https://doi.org/10.1002/macp.202300039.

(55) Taylor, C. J.; Felton, K. C.; Wigh, D.; Jeraal, M. I.; Grainger, R.; Chessari, G.; Johnson, C. N.; Lapkin, A. A. Accelerated Chemical Reaction Optimization Using Multi-Task Learning. *ACS Cent. Sci.* **2023**, *9* (5), 957–968.

https://doi.org/10.1021/acscentsci.3c00050.

(56) Clayton, A. D.; Pyzer-Knapp, E. O.; Purdie, M.; Jones, M. F.; Barthelme, A.; Pavey, J.; Kapur, N.; Chamberlain, T. W.; Blacker, A. J.; Bourne, R. A. Bayesian Self-Optimization for Telescoped Continuous Flow Synthesis. *Angew. Chem.* **2023**, *135* (3), e202214511. https://doi.org/10.1002/ange.202214511.

(57) Houben, C.; Peremezhney, N.; Zubov, A.; Kosek, J.; Lapkin, A. A. Closed-Loop Multitarget Optimization for Discovery of New Emulsion Polymerization Recipes. *Org. Process Res. Dev.* **2015**, *19* (8), 1049–1053. https://doi.org/10.1021/acs.oprd.5b00210.

(58) Knox, S. T.; Parkinson, S. J.; Wilding, C. Y. P.; Bourne, R. A.; Warren, N. J. Autonomous Polymer Synthesis Delivered by Multi-Objective Closed-Loop Optimisation. *Polym. Chem.* **2022**, *13* (11), 1576–1585. https://doi.org/10.1039/D2PY00040G.

(59) Wakiuchi, A.; Takasuka, S.; Asano, S.; Hashizume, R.; Nag, A.; Hatanaka, M.; Miyao, T.; Ohnishi, Y.; Matsubara, T.; Ando, T.; Sugawara, T.; Fujii, M.; Ajiro, H. Composition Regulation by Flow Copolymerization of Methyl Methacrylate and Glycidyl Methacrylate with Free Radical Method. *Macromol. Mater. Eng.* **2023**, *308* (6), 2200626. https://doi.org/10.1002/mame.202200626.

(60) Takasuka, S.; Oikawa, S.; Yoshimura, T.; Ito, S.; Harashima, Y.; Takayama, T.; Asano, S.; Kurosawa, A.; Sugawara, T.; Hatanaka, M.; Miyao, T.; Matsubara, T.; Ohnishi, Y.; Ajiro, H.; Fujii, M. Extrapolation Performance Improvement by Quantum Chemical Calculations for Machine-Learning-Based Predictions of Flow-Synthesized Binary Copolymers. *Digit. Discov.* **2023**, *2* (3), 809–818. https://doi.org/10.1039/D2DD00144F.

(61) Garnett, R. *Bayesian Optimization*; Cambridge University Press, 2023.

(62) *Polymer Handbook Fourth Edition*; Brandrup, J., Immergut, E. H., Grulke, E. A., Eds.; WileyInterscience: New York, 1999.

(63) Balandat, M.; Karrer, B.; Jiang, D. R.; Daulton, S.; Letham, B.; Wilson, A. G.; Bakshy, E. BOTORCH: A Framework for Efficient Monte-Carlo Bayesian Optimization.

(64) Friedman, J. H. Greedy Function Approximation: A Gradient Boosting Machine. *Ann. Stat.* **2001**, *29* (5). https://doi.org/10.1214/aos/1013203451.

(65) Kumar, A.; Pant, K. K.; Upadhyayula, S.; Kodamana, H. Multiobjective Bayesian Optimization Framework for the Synthesis of Methanol from Syngas Using Interpretable Gaussian Process Models. *ACS Omega* **2023**, *8* (1), 410–421. https://doi.org/10.1021/acsomega.2c04919.

(66) Gaonkar, A.; Valladares, H.; Tovar, A.; Zhu, L.; El-Mounayri, H. Multi-Objective Bayesian Optimization of Lithium-Ion Battery Cells for Electric Vehicle Operational Scenarios. *Electron. Mater.* **2022**, *3* (2), 201–217. https://doi.org/10.3390/electronicmat3020017.

(67) Kershaw, O. J.; Clayton, A. D.; Manson, J. A.; Barthelme, A.; Pavey, J.; Peach, P.; Mustakis, J.; Howard, R. M.; Chamberlain, T. W.; Warren, N. J.; Bourne, R. A. Machine Learning Directed Multi-Objective Optimization of Mixed Variable Chemical Systems. *Chem. Eng. J.* **2023**, *451*, 138443. https://doi.org/10.1016/j.cej.2022.138443.

(68) Hanaoka, K. Comparison of Conceptually Different Multi-Objective Bayesian Optimization Methods for Material Design Problems. *Mater. Today Commun.* **2022**, *31*, 103440. https://doi.org/10.1016/j.mtcomm.2022.103440.

(69) Iwasaki, Y.; Jaekyun, H.; Sakuraba, Y.; Kotsugi, M.; Igarashi, Y. Efficient Autonomous Material Search Method Combining *Ab* Initio Calculations, Autoencoder, and Multi-Objective Bayesian Optimization. *Sci. Technol. Adv. Mater. Methods* **2022**, *2* (1), 365–371. https://doi.org/10.1080/27660400.2022.2123263.